 DOI: 10.1002/masy.200650724

Maleic Anhydride Polyethylene Octene Elastomer Toughened Polyamide 6/Polypropylene Nanocomposites: Mechanical and Morphological Properties

Azman Hassan,[*1] *Norhayani Othman,*[1] *Mat Uzir Wahit,*[1] *Lim Jian Wei,*[1] *Abdul Razak Rahmat,*[1] *Zainal Ariffin Mohd Ishak*[2]

Summary: A series of polyamide 6/polypropylene (PA6/PP) blends and nanocomposites containing 4 wt% of organophilic modified montmorillonite (MMT) were designed and prepared by melt compounding followed by injection molding. Maleic anhydride polyethylene octene elastomer (POEgMAH) was used as impact modifier as well as compatibilizer in the blend system. Three weight ratios of PA6/PP blends were prepared i.e. 80:20, 70:30, and 60:40. The mechanical properties of PA6/PP blends and nanocomposite were studied through flexural and impact properties. Scanning electron microscopy (SEM) was used to study the microstructure. The incorporation of 10 wt% POEgMAH into PA6/PP blends significantly increased the toughness with a corresponding reduction in strength and stiffness. However, on further addition of 4 wt% organoclay, the strength and modulus increased but with a sacrifice in impact strength. It was also found that the mechanical properties are a function of blend ratio with 70:30 PA6/PP having the highest impact strength, both for blends and nanocomposites. The morphological study revealed that within the blend ratio studied, the higher the PA6 content, the finer were the POEgMAH particles.

Keywords: mechanical properties; nanocomposites; polyamide 6/polypropylene; polyethylene octene elastomer; toughened polymers

Introduction

In recent years, interest on polymer blends based on engineering polymers such as polyamide 6 (PA6) with polypropylene (PP) had been on the increase. Blending PA6 with PP leads to materials with improved chemical and moisture resistance, dimension stability and reduced cost [1–10]. However PA6 and PP are immiscible and form heterogeneous systems due to different polarities between the two polymers. A number of studies have been reported on the effort to improve the compatibility between PA6 and PP using PPgMAH [1–4]. Besides PPgMAH, maleated rubbers such as EPRgMAH, SEBSgMAH, and EPDMgMAH are also used as compatibilizers in PA6/PP blends [5–10]. Maleic anhydride in the maleated rubbers can react with the end groups of PA6 to form graft copolymer, which act as compatibilizer that helps to distribute the dispersed phase in the matrix phase and to strengthen the PA6-PP interface. Besides acting as compatibilizers, maleated rubbers can also function as toughening agent or impact modifier.

It is well established that rubber toughening is accompanied by a reduction in

[1] Faculty of Chemical and Natural Resources Engineering, Universiti Teknologi Malaysia, 81310 Skudai, Johor Bahru, Malaysia
Fax: +07-5581463.
E-mail: azman61@gmail.com
[2] School of Materials and Mineral Resources Engineering, Universiti Sains Malaysia, Engineering Campus, 14300 Nibong Tebal, Penang, Malaysia

material strength and stiffness. The inclusion of rigid filler on the other hand leads to compensation in stiffness and strength that was sacrificed after the incorporation of elastomeric materials. Polymer nanocomposites based on layered clays have received increasing interest lately [3,4,8,11–17]. Nanocomposites exhibit superior properties such as enhanced stiffness and strength, reduced gas permeability and improved flame retardency.

PA6/PP nanocomposites have been studied extensively by previous researchers [4,8,14,18]. The results have shown that the highest tensile and flexural strength values were achieved at 4 wt% organoclay [18]. Ductility also dropped sharply with the incorporation of organoclay. However, little work has been done on toughened PA6/PP nanocomposites. Recently, there has been a considerable interest in polyethylene octene elastomer (POE), which is a relatively new metallocene elastomer due to faster mixing and better dispersion when blended with PP compared with conventional polyolefin elastomer [9,10]. This paper focuses on the effects of POEgMAH as compatibilizer and impact modifier on the mechanical and morphological properties of PA6/PP nanocomposites.

Materials and methods

Materials

The blends used in this work are described in Table 1. The PA6 (Amilan CM 1017) was a commercial product from Toray Nylon Resin AMILAN, Japan. The MFI of PA6 is 35 g/10 min at 230 °C and 2.16 kg load and the density is 1.14 g/cm^3. The PP (SM 240) was obtained from Titan PP Polymers, Johor Bahru, Malaysia. The melt flow index (MFI) and density of PP is 25 g/10 min (at 230 °C and 2.16 kg load) and 0.9 g/cm^3 respectively. Polyethylene octene random (11 wt% octene) copolymer grafted with maleic anhydride of DuPont (Fusabond MN493D) with density 0.87 g/cm^3 was supplied by DuPont Dow Elastomers. Two different grades of organoclay were used in this study. These organoclay are a white powder containing montmorillonite (MMT) (70 wt%) intercalated by octadecylamine (30 wt%). They are i. Nanomer 1.30 TC, which is suitable for use in polyamide resin and ii. Nanomer 1.30 P, a surface modified MMT minerals intercalated by stearyl ammonium chloride, which is suitable for use in polyolefin resins. Both organoclays are commercial products from Nanocor Inc. USA.

Specimen Preparation

PA6, PP, POEgMAH and organoclay were dry blended in tumbler mixer according to the composition in Table 1. The polymers and additives were then melt blended by simultaneous addition for all components into a Berstoff co-rotating twin screw extruder. The barrel temperatures were gradually increased from hopper to die at 200, 220, 230 and 240 °C and the rotating screw was 50 rpm. Prior to extrusion, PA6 pellets were dehumidified by using a dryer at 80 °C for 8 hours. The pelletized materials were dried and injection molded into a standard specimen for mechanical tests.

Materials Characterization

Mechanical Testing

Flexural test were carried out according to ASTM D790 method using an Instron 5567 Universal Testing Machine under ambient condition. The crosshead speed for flexural test was set at 3 mm/min. The Izod impact test was carried out on notched specimens using Toyoseiki impact tester at ambient condition according to ASTM D256. The values reported in this study are the average of five specimens tested.

Microscopy Examination (SEM)

The morphology of the blends was examined using a Philips scanning electron microscope. Samples were cryogenically fractured in liquid nitrogen and etched in hot heptane for 5 hours to extract the elastomeric POEgMAH phase. Samples

Table 1.
PA6/PP systems used in this study.

Formulation	PA6	PP	POEgMAH	Organoclay
	(wt%)	(wt%)	(wt%)	(wt%)
Neat polymers				
PA6	100	—	—	—
PP	—	100	—	—
Blends				
PA6/PP (80:20)	80	20	—	—
PA6/PP (70:30)	70	30	—	—
PA6/PP (60:40)	60	40	—	—
POEgMAH toughened polymers				
PA6 E10	90	—	10	—
PP E10	—	90	10	—
POEgMAH toughened blends				
PA6/PP (80:20) E10	72	18	10	—
PA6/PP (70:30) E10	63	27	10	—
PA6/PP (60:40) E10	54	36	10	—
POEgMAH toughened nanocomposites				
PA6 E10FA4	86	—	10	4
PA6/PP (80:20) E10FA4	68.8	17.2	10	4
PA6/PP (70:30) E10FA4	60.2	25.8	10	4
PA6/PP (60:40) E10FA4	51.6	34.4	10	4
PP E10C6FB4	—	86	10	4

were coated with gold prior to examination under the electron beam. An operating voltage of 30kV and a magnification of 1000x were used.

X-ray Diffraction (XRD)

X-ray diffraction was performed with the Siemens XRD. The XRD diffraction patterns were recorded with a step size of 0.02° from $2\theta = 2$ to 10°. The interlayer spacing of organoclay was derived from the peak position (d_{001}-reflection) in XRD diffractograms according to Bragg equation.

Results and Discussion

Mechanical Properties

Figures 1 and 2 show the flexural modulus and strength as a function of weight fraction for all PA6/PP blends, POEgMAH toughened PA6/PP blends and toughened PA6/PP nanocomposites. It can be seen that flexural modulus and strength of all categories of samples followed the same trend. The flexural modulus and strength of samples containing neat PA6 were higher compared to neat PP and decreased with increasing PP weight fraction. This may be attributed to the strength and stiffness of PA6 being higher than PP. According to Ersoy et al. [19] the higher tensile strength of PA6 compared to PP can be attributed to the highly polar nature of PA6 and subsequently the large number of hydrogen bonding interaction, which give rise to the resistance against external forces. A sharp drop in strength and modulus was observed with the incorporation of 30 wt% PP, but the decline was more gradual with further addition of 10 wt% PP.

The results also showed that the flexural modulus and strength were reduced with the incorporation of POEgMAH into the PA6, PP and PA6/PP blends. This is due to the diluting effect of the blends with addition of elastomer. Similar observation was reported by Bai et al. [9]. However, interestingly the addition of organoclay into POEgMAH toughened samples enhanced the flexural modulus and strength of the toughened nanocomposites. The stiffness of silicates layers contributes to the presence of immobilized or partially immobilized polymer phases [12,13]. The high aspect ratio of organoclay resulted in a

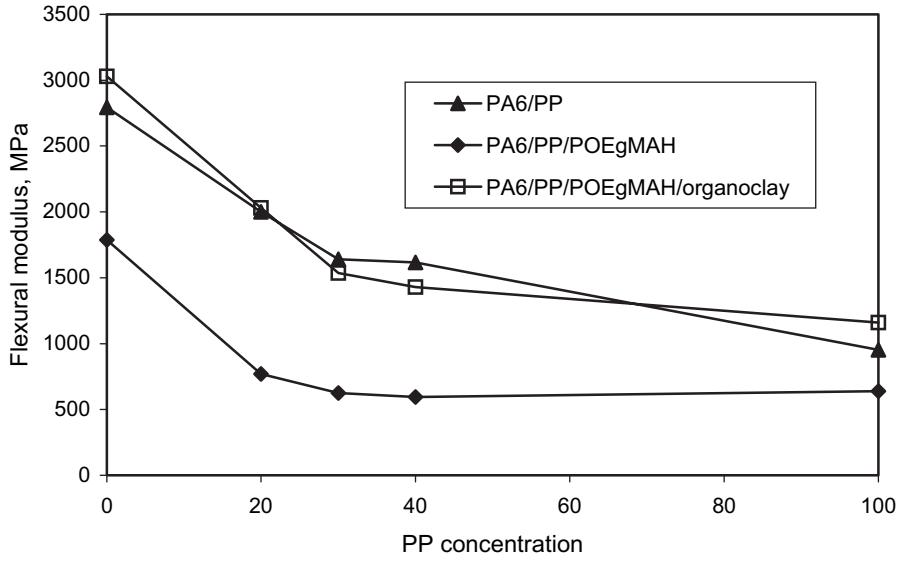

Figure 1.
The effect of PA6/PP blends ratio on flexural modulus.

large contact surface area with polymer matrix also contributes to the observed reinforcement effect. Recently, Chow et al. [4,8] reported that the maleic anhydride group of PPgMAH or EPRgMAH which was used as compatibilizer in their study may react with octadecylamine group from organoclay forming hydrogen bonds. It is believed that the use of POEgMAH in the present study also improved the interfacial

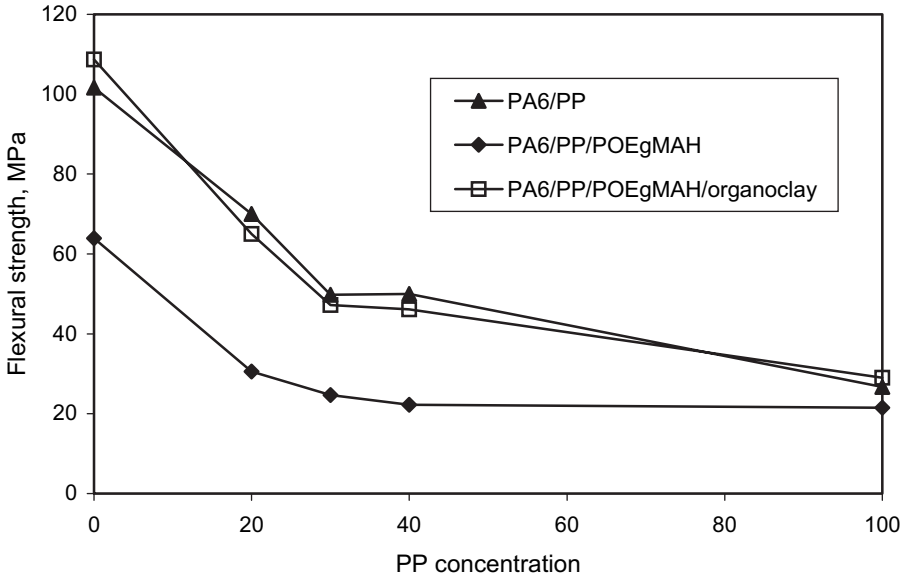

Figure 2.
The effect of PA6/PP blends ratio on flexural strength.

bonding between PA6 and PP, besides favouring a degree of dispersion of organoclay. POEgMAH acts as the driving force during the initial intercalation of the nanoclay. Usuki et al. [16] suggested that the superior mechanical properties of the organoclay nanocomposites materials could be contributed to the strong ionic interaction between matrix and silicate layers. The good interaction between organoclay and matrix may lead to a desired and better dispersion of organoclay in the polymer matrix, resulting in an efficient reinforcement.

As shown in Figure 3 the impact strength of PA6/PP blends was higher than neat PA6 and increased with increasing PP weight fraction until an optimum concentration at PA6/PP (70:30) weight fraction. The results also showed that the POEgMAH increased the impact strength of all samples. Interestingly to note that siginificant imptrovement was observed for all the blends with the PA6/PP (70:30) blends having the highest impact strength values. Holsi-Miettinen et al. [7] and Gonzalez-Montiel et al. [5] reported that higher impact strength was obtained for EPRgMAH or SEBSgMAH toughened PA6/PP when the PA phase was dominant compared to PP dominant. The reason was that the addition of PP as a minor phase activated toughening mechanism that improved the impact strength of PA6/PP blends [7]. Tjong [2] explained that the high impact strength of PA/PP (80:20) was attributed to debonding and cavitation which occured simultaneously at the PP-PA interface and promoted massive shear deformation in the PA matrix. This resulted in an increase in the amount of energy being absorbed. However, the addition of organoclay reduced the impact strength of toughened PA6, PP and PA6/PP blends. For the nanocomposites, the impact strength of PA6/PP (70:30) blend was the highest, similar to that of toughened PA6/PP blend.

Phase Morphology

Figures 4 (a) (b) and 5 (a) (b) show SEM micrographs of freeze-fractured surfaces under liquid nitrogen of toughened blends and toughened nanocomposites of PA6/PP (80:20) blends, PA6/PP (60:40) blends, respectively. The etched surfaces showed dark circular holes which represent the

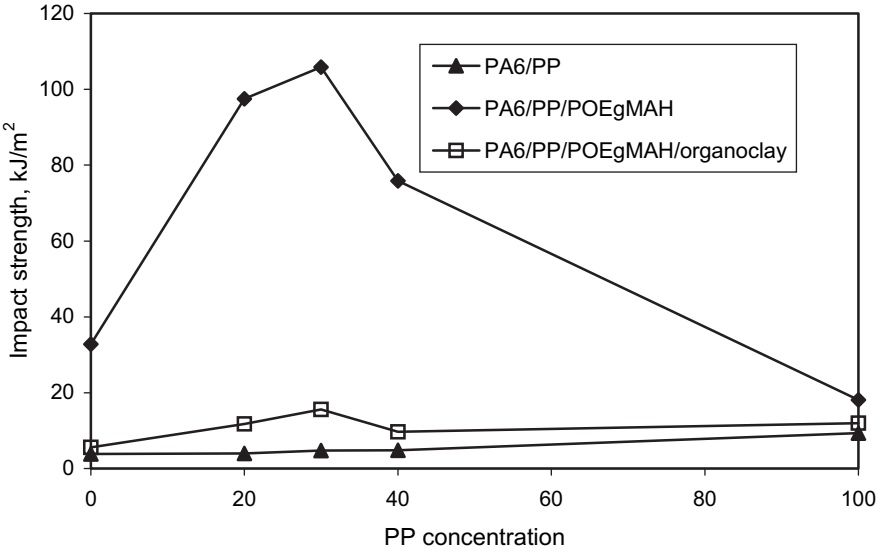

Figure 3.
The effect of blend ratio on impact strength of PA6/PP blends.

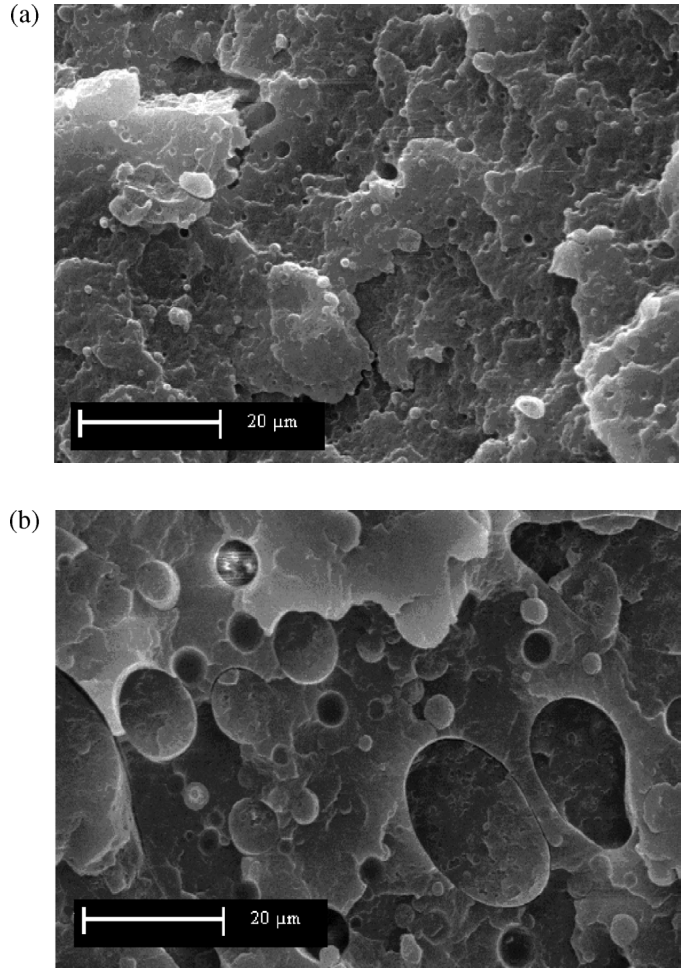

Figure 4.
SEM micrographs of cryo-fractured surfaces extracted by heptane (a) PA6/PP (80:20)/POEgMAH (b) PA6/PP (60:40)/POEgMAH.

POE particles as heptane dissolved only the rubber phase but did not dissolve PA6 or PP. Figure 4 shows that particles size of POEgMAH in PA6/PP (80:20) blends were smaller than in PA6/PP (60:40) blends. This reveals that the compatibility between PA6/PP and POEgMAH rubber increased with increasing PA6 content, as a result of interaction between maleic anhydride group of POEgMAH and PA6. Similar trend was observed in PA6/PP nanocomposites. Comparing Figure 4 and 5 revealed that POEgMAH size in PA6/PP nanocomposites was smaller than PA6/PP. It can be clearly shown that the organoclay does play a dramatic role in reducing the dispersed rubber size in the matrix. Khatua et al. [11] reported similar observation in their study on PA6/EPR nanocomposites where domain size of EPR decreased even when small amount (~1 wt%) of organoclay was added.

The reduction in dispersed domain sizes might be attributed to the changes in rheological properties and barrier effect, which prevent coalescence of dis-

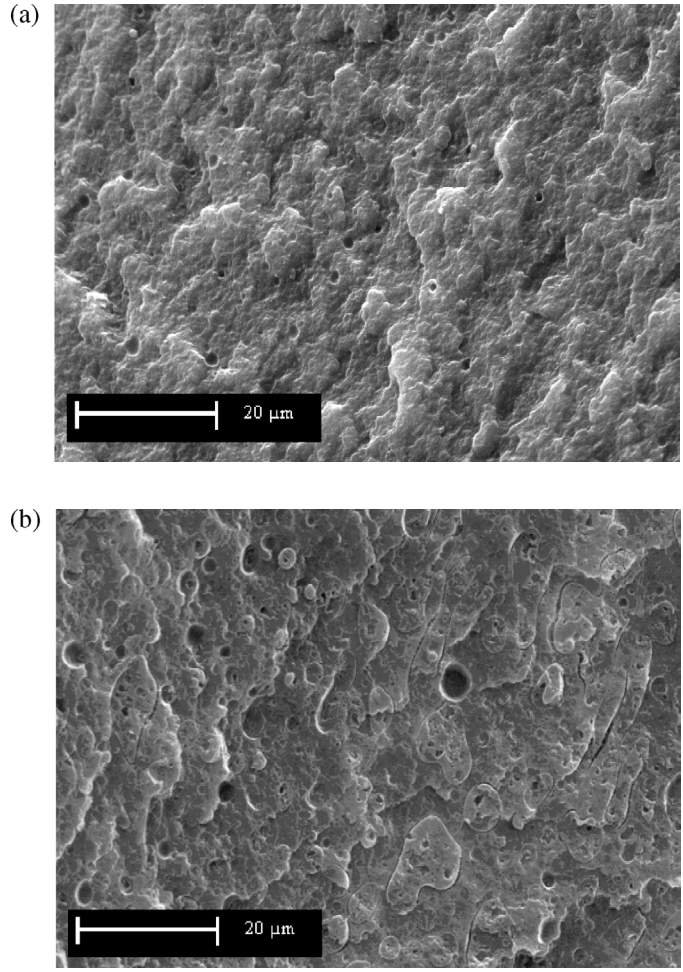

Figure 5.
SEM micrographs of cryo-fractured surfaces extracted by heptane (a) PA6/PP (80:20)/POEgMAH/organoclay (b) PA6/PP (60:40)/POEgMAH/organoclay.

persed phase [11]. As reported by Li and Shimizu [15] the morphological changes in nanocomposites attributed to the effect of clay platelets on the melt behavior of the blends system. The addition of organoclay can increase the viscosity of the polymer matrix due to the strong interaction between the organoclay and the PA6. This would lead to the reduction of melt viscosity difference between continuous polymer matrix and dispersed phase, thus improving the mixing properties of the blends. Besides viscosity changes, high aspect ratio of clay platelets can also act as barriers to effectively prevent the coalescence of dispersed phase.

XRD Characterization

Figure 6 and Figure 7 show the X-ray diffraction patterns of organoclay, toughened PA6, PP and PA6/PP blends nanocomposites as a function of PP weight fraction. X-ray parameters calculated from the (001) peaks are summarized in Table 2. From the XRD diffractogram in Figure 6, it can be seen that the XRD patterns of the

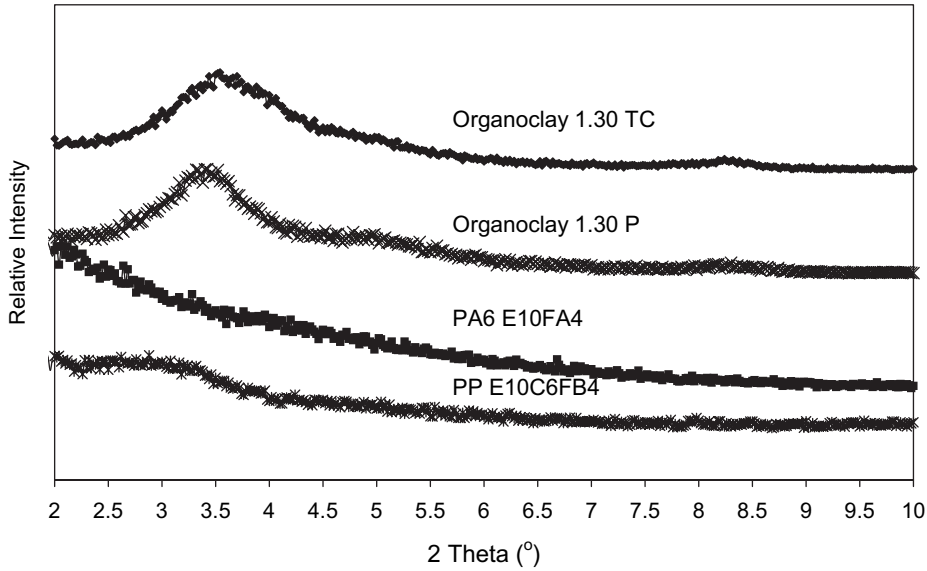

Figure 6.
XRD patterns for the organoclay, toughened PA6 nanocomposites and toughened PP nanocomposites.

organoclay 1.30 TC exhibited a broad intense peak at around $2\theta = 3.52^\circ$ corresponding to a basal spacing of 2.48 nm, whereas for organoclay 1.30 P it was about 2.59 nm ($2\theta = 3.40^\circ$). For toughened PP nanocomposites the characteristic (001) peak of the organoclay was shifted to $2\theta = 2.82^\circ$ (corresponding to a basal spacing of 3.13 nm). This indicates that some PP and POEgMAH molecular chains were

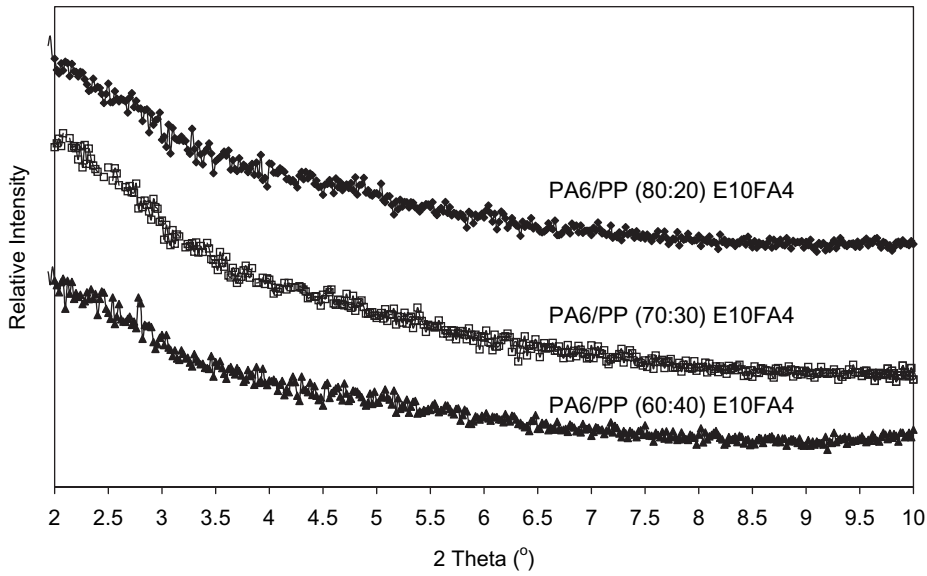

Figure 7.
XRD patterns for the toughened PA6/PP nanocomposites with different PA6/PP blends ratio.

Table 2.
XRD parameters of organoclay, toughened PA6, PP and PA6/PP blends nanocomposites

Sample	2θ(°)	d(nm)
Organoclay (1.30 TC)	3.52	2.48
Organoclay (1.30 P)	3.40	2.59
PA6 E10FA4	Not detected	Not detected
PA6/PP (80:20) E10FA4	Not detected	Not detected
PA6/PP (70:30) E10FA4	Not detected	Not detected
PA6/PP (60:40) E10FA4	Not detected	Not detected
PP E10C6FB4	2.64	3.35

intercalated between the clay galleries forming an intercalated structure during the direct melt blending process.

On the other hand, the XRD patterns did not show any organoclay diffraction peak for toughened PA6 nanocomposites, suggesting that the organoclay platelets were completely exfoliated in the PA6 matrix, which is consistent with previous researches on PA nanocomposites [3,12,14–16]. Similar trend is also observed in the PA 6 dominant toughened PA6/PP nanocomposites where no diffraction peak was detected (Figure 7). This result indicates that the organoclay were delaminated and has a higher affinity with PA6 than PP, where intercalation of the non-polar macromolecule segments of PP into interlayers of the organoclay is not as effective as compared to PA6. Therefore the organoclay may selectively be located in the PA6 phase. The organoclay layers are easily exfoliated by PA6 molecular chain compared to PP molecular chain because of the higher polarity of the PA6 chain. The above observations show that the nanostructure depends on the interaction between the polymer chain and the organoclay. The hydroxyl group and oxygen atoms on the organoclay surface make the organoclay more compatible with polar polymer [3]. This is why PA6 has better interaction with the organoclay as compared to PP.

As reported by Yoo et al. [14] on PA6/LLDPE nanocomposites with various compositions, as PA6 content increase the interlayer distance of the organoclay were increased. They also concluded that the amount of PA6 is a significant factor in determining the interlayer distance of the organoclay due to its polar characteristic. In other words, the organoclays might selectively locate in the PA6 phase rather than LLDPE phase due to the organoclay having more affinity to PA6.

Conclusion

The mechanical behaviour of PA6/PP blends, toughened PA6/PP and toughened PA6/PP nanocomposites depends on the proportion of the constituents. The impact strength of the PA6/PP increased with the incorporation of POEgMAH but at the expense of strength and stiffness. Incorporation of organoclay into the toughened PA6/PP led to the enhancement in flexural modulus and strength but decreased the toughness. Blends of PA6/PP with 70:30 showed the highest impact strength for both toughened blends and nanocomposites. SEM observation on the cryogenic surface revealed that the POEgMAH particles size decreased with the incorporation of organoclay and with increasing PA6 content for PA6/PP blends and PA6/PP nanocomposites. XRD showed that the exfoliated nanocomposite were formed in PA6 and PA6 dominant system.

[1] F.P. Tseng, J.J. Lin, C.R. Tseng, F.C. Chang, *Polymer* **2001**, 42, 713.
[2] S.C. Tjong, *Journal of Materials Science* **1997**, 32, 4613.
[3] H. Wang, C. Zeng, M. Elkovitch, L.M. Lee, *Polymer Engineering and Science*. **2001**, 41, 2036.
[4] W.S. Chow, Z.A. Ishak, J.K. Kocsis, A.A. Apostolov, U.S. Ishiaku, *Polymer* **2003**, 44, 7427.
[5] A. Gonzalez-Montiel, H. Keskkula, D.R. Paul, *Polymer* **1995**, 36, 4605.
[6] S.C. Wong, Y.W. Mai, *Polymer* **1998**, 40, 1553.
[7] R.M. Holsti-Miettinen, J.V. Seppala, O.T. Ikkala, I.T. Reima, *Polymer Engineering and Science* **1997**, 34, 395.
[8] W.S Chow, Z.A. Ishak, J.K. Kocsis, A.A. Apostolov, U.S. Ishiaku, *European Polymer Journal* **2005**, 41, 687.
[9] S.L. Bai, G.T. Wang, J.M. Hiver, C. G'Sell, *Polymer* **2004**, 45, 3063.
[10] N. Zeng, S.L. Bai, C.G. Sell, J.M. Hiver, Y.W. Mai, *Polymer International* **2002**, 51, 1439.

[11] B.B. Khatua, D.J. Lee, H.Y. Kim, J.K. Kim, *Macromolecules* **2004**, 37, 2454.
[12] T. Liu, Z.H. Liu, K.X. Ma, L. Shen, K.Y. Zeng, C.B. He, *Composites Science and Technology* **2003**, 63, 331.
[13] X. Liu, Q. Wu, *Polymer* **2001**, 42, 10013.
[14] Y. Yoo, C. Park, S.G. Lee, K.Y. Choi, D.S. Kim, J.H. Lee, *Macromolecular Chemistry and Physics* **2005**, 206, 878.
[15] Y. Li, H. Shimizu, *Polymer* **2004**, 45, 7381.
[16] A. Usuki, A. Koiwai, Y. Kojima, M. Kawasumi, A. Okada, T. Kurauchi, O. Kamigaito, *Journal of Applied Polymer Science* **1995**, 55, 119.
[17] W. Xu, G. Liang, W. Wang, S. Tang, P. He, W.P. Pan, *Journal of Applied Polymer Science* **2003**, 88, 3225.
[18] W.S. Chow, Z.A. Ishak, J.K. Kocsis, A.A. Apostolov, U.S. Ishiaku, *Journal of Applied Polymer Science* **2004**, 91, 175.
[19] O.G. Ersoy, N. Nugay, *Polymer Bulletin* **2003**, 49, 465.

